2016

Rapid detection of theophylline using an aptamer-based nanopore thin film sensor

Silu Feng
Iowa State University

Rapid detection of theophylline using an aptamer-based nanopore thin film sensor

by

Silu Feng

A thesis submitted to the graduate faculty

in partial fulfillment of the requirement for the degree of

MASTER OF SCIENCE

Major: Electrical Engineering

Program of Study Committee:
Long, Que, Major Professor
Wei Wang
Santosh Pandey

The student author and the program of study committee are solely responsible for the content of this thesis. The Graduate College will ensure this thesis is globally accessible and will not permit alterations after a degree is conferred.

Iowa State University

Ames, Iowa

2017

DEDICATION

I would like to dedicate this thesis to my parents Bangming Feng and Lanying Wang. Without their unconditional love and financial support, I would not have been able to complete this work.

I would like to dedicate this thesis to my super adviser: Long Que. Without his help, I would not achieve my goal.

I would like to dedicate this thesis to my Yiyi Sun, Xiong Deng and Lin Kong who have always being there for me.

TABLE OF CONTENTS

Page

LIST OF FIGURES

LIST OF TABLES

Page

ABSTRACT

This paper reports, *for the first time*, an aptamer-based nanopore thin film sensor for detecting the ophylline in buffer and complex fluids. In my experiments, I created the sensor and found that it could help us to better test theophylline than an antibody-based detection sensor. The following is a detailed explanation of the sensor creation and the experimental process.

Anodic aluminum oxide (AAO) has been investigated and applied in numerous products since the 1970s. It is a highly-arrayed porous nanostructure as shown in Figure 1. The pore size normally ranges from tens to hundreds of nanometers, and the aspect ratio could be higher than 40:1. Application areas of AAO include biomedical sensing, energy storage, template-based nanofabrication, electronics, etc. In my experiment, I applied AAO to the process of creating a sensor.

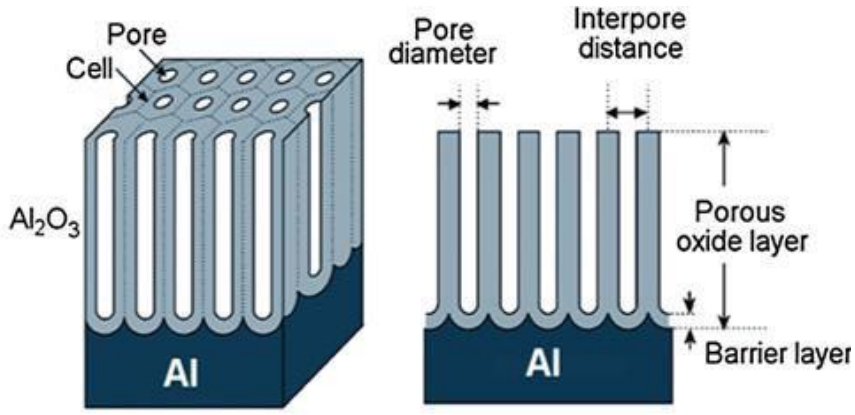

Figure 1. The structure of AAO

In my experiments, I chose RNA aptamer rather than antibodies because its molecules overcome the weakness of antibodies. The 33 nts RNA aptamer sequences used were found to recognize and selectively bind theophylline (Figure 2) [1]. Moreover, aptamers are easy to synthesize, have both excellent heat stability and a wide tolerance range of PH and salt

concentration, and is much less costly than antibodies.

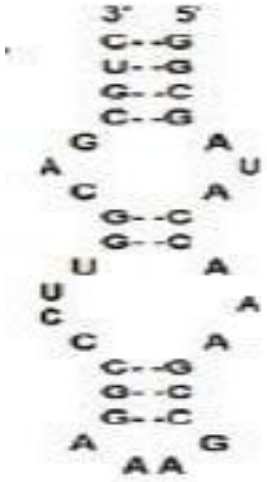

Figure 2. Theophylline-binding RNA aptamer seuqence

The first study used an aptamer-based nanopore thin film sensor to detect theophylline in the buffer and complex fluids. I first fabricated the nanopore thin film sensors with a microfluidic interface, then demonstrated the surface functionalization procedure of the sensor. I then used optical transducing signals to detect the fringes followed by using the sensor as a reference sensor to further cancel out the non-specific binding effect; theophylline in low concentration (0.2μM), caffeine, theobromine, and plant extract were successfully detected. The experiment showed that this aptamer-based sensor had good specificity and selectivity, allowing me to further test theophylline in serum.

The second study used an optical aptamer-based plant hormone sensor with a microfluidics capillary interface. I adopted the exact same methodology and sensor from themy first study and further designed an optical aptamer-based sensor with a microfluidics capillary interface to upgrade the testing process. Such a microfluidics capillary interface allows samples to be automatically delivered to the sensor without use of external pumps.

This explains how the aptamer-based nano thin film censor was created and how my two

successful experiments were performed. The research outcome is that an aptamer-based label-free sensor for optically detecting theophylline has been demonstrated for the first time. It performs much better than its competitors and has a promising future in further applications in similar experiments.

CHAPTER 1. GENERAL INTRODUCTION

Research Motivation

Theophylline (TP) is a drug used for treatment of respiratory diseases such as asthma through its bronchodilatory effects [2], but TP levels within the body must be quickly and regularly monitored since it has a narrow safety range, i.e., within 20μM to 100μM [3].People usually use blood samples to monitor TP levels in current clinical practice; is very important to monitor theophylline level in blood because it is toxic at higher levels and can cause severe and protracted vomiting , acute overdose, chronic overdose, sustained-release preparation, immediate-release preparation, and permanent neurological damage.

Current widely-used laboratory procedures for theophylline detection include radioimmunoassay [4], high performance liquid chromatography [5], and fluorescence polarization immunoassay [6], all of which suffer from interference, primarily from structurally closely related caffeine and theobromine that can result in overestimated serum/plasma theophylline concentrations. These methods also require skilled personnel, sample pre-treatment, and long analysis times [1]. Current laboratory procedures use antibody-based sensing to detect the theophylline. This type of sensing exhibits some weaknesses such as being labor-intensive, very expensive, and easily susceptible to irreversible denaturation[7].

To address these issues, we introduce a new type of aptamer-based label-free sensor for optically detecting theophylline to be reported and demonstrated for the first time. The advantages of our method include good selectivity, specificity, high stability, and cost-effectiveness.

Thesis Organization

Chapters 2 and 3 discuss the research goals outlined above. Chapter 2 specfically describes the operational principles of aptamer-based nanopore thin film sensors, sensor fabrication, and the experimental procedure used. Chapter 2 also describesresultsrelated to detectionof concentrations of theophylline in caffeine, theobromine, and plant extract.

Chapter 3 describes further experiments in testing the concentration of theophylline for 0.2μM, 1μM, 2μM, 4μM, 8μM, 16μM, 32μM and 48μM. Each concentration test was repeated I 5 times, followed by testing 0μM, 4μM, 40μM theophylline dissolved in Newborn Calf Serum.

Chapter 4 describes the design and the process flow used to fabricate the sensor. Appendix A gives more details regarding the principle underlying the process of surface functionalization and detection and provides a more detailed description of the nanopore thin film sensor fabrication process. Appendix B provides a schematic view of four masks. Appendix C gives fabrication details of the AAO.

References

[1] E.E. Ferapontova, E.M. Olsenand K.V. Gothelf, "An RNAaptamer- based electrochemical biosensor for detection of the ophyllineinserum," J.Am.Chem. Soc., vol. 130, pp: 4256–4258,2008.

[2] P.J.Barnesand R.A.Pauwels, "Theophylline in the man agement of asthma: time for reappraisal?"Eur.Respir.J.,1994,vol.7,pp.579–591,1994.

[3] A.H.DawsonandI.M. Whyte, "Therapeutic drugmoni to ring in drug overdose,"Br.J.Clin.Pharmacol.,vol.48,pp:278–283,1999.

[4] C.E. Cook,M. E.Twine,M. Myers, E. Amerson,J. A. Keplerand G. F.Taylor, "The ophylline

radioimmunoassay: synthesis of antigen and characterization of antiserum,"Res.Commun.Chem.Pathol.Pharmacol.,vol.13,pp:497–505,1976.

[5] B.Srdjenovic,V.Djordjevic-Milic,N.Grujic,R.InjacandZ.Lepojevic, "Simultaneous HPLCD etermination of Caffeine, The obromine, and The ophyllinein Food, Drinks, andHerbal Products,"J.Chromatogr.Sci., vol.46,pp:144–149,2008.

[6] M.E. Jolley, "Fluorescencepolarizationimmunoas say for determination of therapeutic drug level sinhumanplasma,"J.Anal.Toxicol.,vol.5,pp: 236–240,1981.

[7] K.Song,S.Lee, and C.Ban."Aptamers and their biological applications."

CHAPTER 2. RAPID DETECTION OF THEOPHYLLINE USING AN APTAMER-BASED NANOPORE THIN FILM SENSOR

Modified from a paper submitted to IEEE-Sensors

Silu Feng, Xiangchen Che, Long Que, Changtian Chen, Wei Wang

Abstract

This paper reports, *for the first time*, an aptamer-based nanopore thin film sensor for detecting theophylline in buffer and complex fluids. Compared to antibody-based detection, aptamer-based detection offers many advantages such as low cost and high stability a t elevated temperatures. Experiments found that this type of sensor, without any optimization, can detect the theophylline at a concentration as low as 0.2μM, which is comparable to the detection limit of current lab-based equipment such as liquid chromatography(LC). Experiments also demonstrated that the aptamer-based sensorh as good specificity and selectivity. By using some nanopore thin film sensors as there ference sensors to further can celout the non-specific binding effect, the theophylline in plant extract as been detected successfully.

Introduction

Theophylline(TP) is a drug used for treatment of respiratory diseases such as asthma due to its bronchodilatory effects [1]. But the TP levels with in the body should be monitored quickly and regularly since it as a narrow safety range[2].For instance, blood samples from patients are usually used to monitor the TP levels in current clinic practice. However, such blood samples are each usually in excess of25 mL, and more than one sample is required for the tests. Hence it becomes problematic for patients to provide the se regular blood samples. Since it is very

important to monitor theophylline level in blood because of its toxicological effects, ideally a sensor, which can detect the theophyllineon-site with small sample sizes(<100μL or lower), becomes increasingly critical.

Current widely-used laboratory procedures for theophylline detection include radioimmunoassay[3], highper for mance liquid chroma to graphy [4],and fluorescence polarization immunoassay [5], but the methods usually require skilled personnel, sample pre-treatment, and long analysis times. To address the issues, different types of sensors have been developed. Examples include studying the electrochemical oxidation of the theophylline by using a variety of electrode substrates [6-7]. All these reported technologies have their own advantages and disadvantages.

The use of antibody-based sensing has been available for more than three decades. In recent years, aptamers are widely known as a substitute for antibodies, because the some molecules over come the weaknesses of antibodies[8]. Specifically, aptamers have very good heat stability, easeofsyn thesis, cost-effectiveness, and a wide tolerance range of pH and salt concentration. On the other hand, aptamers offer a similar, if not better, specificity and affinity to antibodies. Finally, aptamers can also be being reversibly denatured for the release of target molecules. All these features make them perfect receptors for biosensing applications. Herein, a new type of aptamer-based label-free sensor for optically detecting the theophylline is reported and demonstrated *for the first time*.

Principle of the aptamer-based sensor

The sketch and operational principles of the aptamer-based nanopore thin film sensor are illustrated in **Fig.3**. The nanopore thin film is basically anodicaluminum oxide(AAO). Inside AAO thin film there are periodically distributed nanopores [9]. Typical size of then a nopore

can be from 20nm to150nm. Both nanopore size and the interspace among nanopores can be adjusted readily by modifying the process parameters for fabricating AAO during the anodization step. To detect theophylline, the AAO nanopore surface of each sensoris functionalized with the theophylline-binding RNA aptamer. Since the RNA aptameris theophylline specific, it can only capture the theophylline. The optical signal (interference fringes) from the sensor under goes variation when the theophylline is bound to the aptamer. More specifically, as shown in **Fig.3**, the optical interference fringes reflected from the sensor, the transducing signal of the sensor, result in shift before and after the theophylline is bound to the aptamer[10-11].

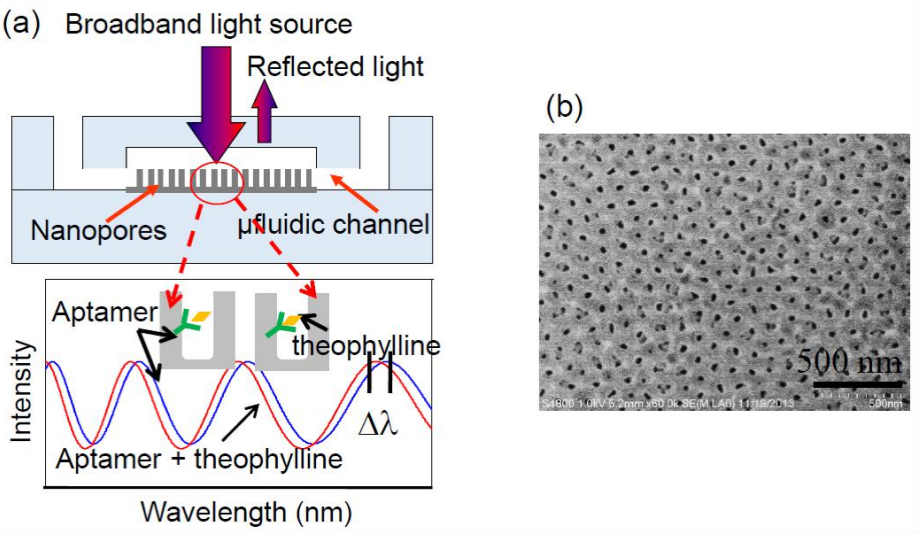

Figure 3**. (a) Sketch and operational principle of an aptamer-based nanopore thin film sensor; (b) SEM image of the AAO nanopores in the thin film**

Sensor fabrication and experimental procedure

Sensor fabrication

The sensor was fabricated using the process flow developed in our lab, described in detail in citation [9]. The basic process flow is illustrated in **Fig. 4(top)**. Briefly, after a 5-minute

baking of the rigorously cleaned cover slip glass substrate, an aluminum (99.999%) layer about 2-3 μm thick is deposited by E-beam evaporation. Then a one-step anodization process in acid solution (0.3 M oxalic acid) with 45 V DC voltage at 2 °C to form AAO on the glass substrate is carried out as shown in Fig. 2(top-c). As a result, a layer of AAO is formed on the whole glass substrate. Thereafter, photolithography is performed on the Al-coated AAO substrate. The patterns are then transferred to the Al layer by etching the unprotected Al area in an etching solution {(H_3PO_4:CH_3COOH:HNO_3:H_2O) 80:5:5:10 by weight %} for 35 s. The patterned Al thus is used as the mask, the substrate is immersed in a mixture of phosphoric acid (0.4 M) and chromic acid (0.2 M) at 20 °C for 100 minutes to etch away the unprotected AAO and transfer the Al patterns into the AAO layer. Finally, the Al is etched away, and then AAO nanopore thin film sensors are fabricated after a layer of 10 nm Au is coated on AAO surface.

A photo of a fabricated chip consisting of 15AAO nanopore thin film sensors with a microfluidic interface is shown in Fig.4(middle).

Surface functionalization and detection

The Au-coated sensor surface is functionalized with the theophylline aptamer through 1-ethyl-3-(3- dimethylaminopropyl) carbodiimide (EDC)/N- hydroxysulfosuccinimide (NHS) chemistry as shown in **Fig.4(bottom)**.More specifically, the Au-coated sensor surface is immersed in the10mM$HSC_{10}COOH$/HSC_8OH solution for 30min and then washed with ethanol and DIwater. After the surface is dried, the surface is immersed in a solution of NHS and EDC (NHS0.2M,EDC 0.05M)for30min. Thes ensor surface is then washed with DI water

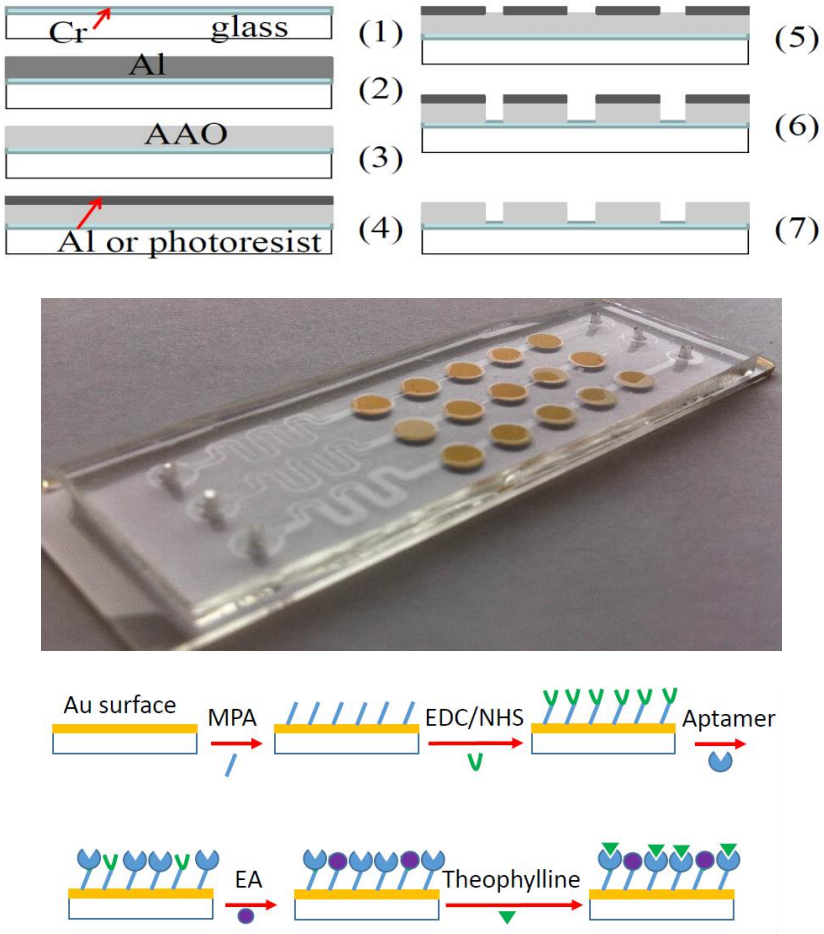

Figure 4. (top) Fabrication process flow of the nanopore thin film sensor; (middle) photo of 15 fabricated nanopore thin film sensors with microfluidic interface; and (bottom) illustration of the surface functionalizaion procedure of the sensor

and then immersed in the 5μM aptamer solution over night. This is followed by loading of 100μL1 Methanolamine (EA)to block then on-occupied MPA sites activated by theEDC/ NHS, followed by aninjectionof 100 μL of 100mM phosphoric acid(PPA) to remove then on-specific binding. Finally, the sensor surface is rinsed with the PBS buffer to flush off non-specifically adsorbed proteins. At this stage, the sensor is ready for them measurement.

For all there ported measurements in the following section, after the samples are applied to the sensor and incubated for 30-50 min, a three-time vigorousrinsein a running PBS buffer

to remove the unbound samples on the sensor surface is carried out, followed by three optical measurements. The results are the average values from the three measurements.

Results and discussion

Typical optical transducing signals from a sensor before and after applying the theophylline (TP) are shown in **Fig. 5**. In this case, the theophylline is in PB buffer. The optical interference fringes exhibit clear shift. As expected, the higher the concentration of the theophylline, the larger shift of the fringes. Note that no further shift can be observed once the binding sites of the aptamer have been totally occupied by theophylline. For current sensor without any design changes, up to 100 µM of theophylline can be detected.

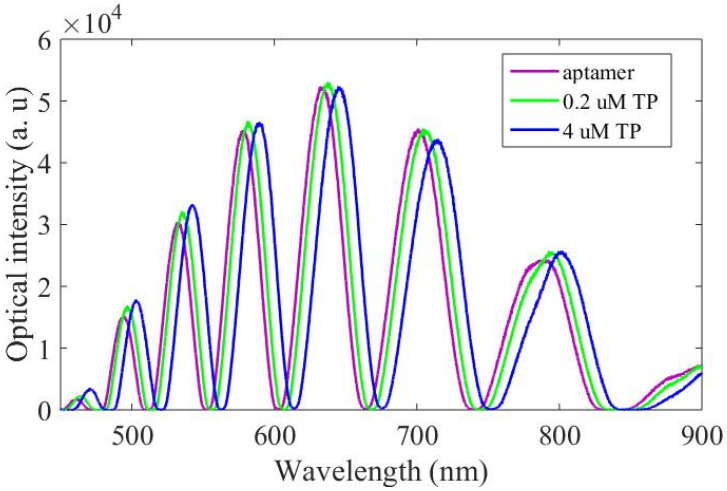

Figure 5. Typical measured optical signals for theophylline (TP) in PBS buffer at concentrations of 0.2 µM and 4 µM: interference fringes' shift increases with TP concentration

On the other hand, it has been found that the concentration of the theophylline of 0.2 µM

can be detected readily by the sensor (**Fig. 5**). This concentration is closed to the detection limit of current equipment such as liquid chromatography. Note that the detection limit of the sensor can be further improved by modifying the nanopore size and density, which is under investigation in our lab.

The specificity of the sensor has also been evaluated. In this case, instead of applying theophylline, caffeine and theobromine, usually associated with theophylline, are applied on the sensor. For instance, the measured optical signals for theobromine(TB) are given in **Fig. 6**. As can be seen, the fringes shift is ~0.15 nm when only theobromine is applied. In contrast, the fringes shift is much more pronounced about ~4.0 nm when 40 μM theophylline is added to the theobromine solution. Similar results have been obtained for caffeine, suggesting the good specificity of the aptamer-based assay.

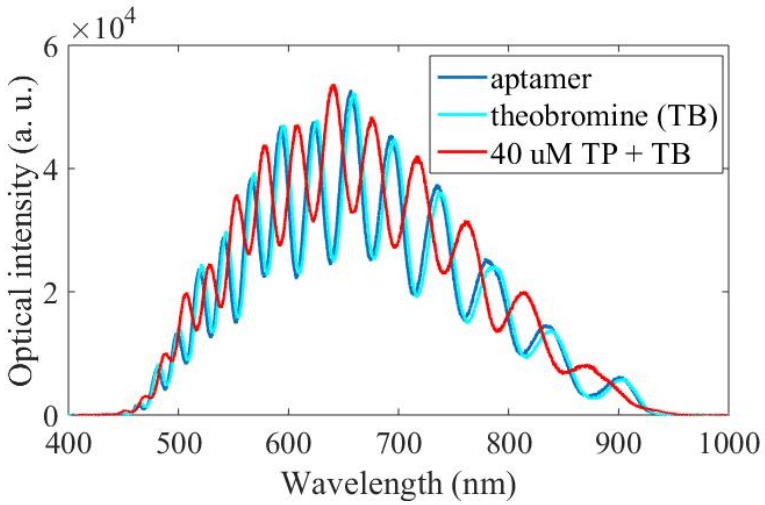

Figure 6. Measurements for non-specific binding result for theobromine (TB), concentrations of theophylline in theobromine of 0 μM and 40 μM.

However, even though the non-specific binding for both theobromine and caffeine is small, but the optical fringe shift still exists. In order to further cancel out the non-specific binding effect in the measurements, first, the reference sensor is used to calibrate the shift due to the non-specific binding. Then, the pure shift due to the theophylline is obtained by

subtracting the shift of the reference sensor from the measurements of the theophylline in complex fluids.

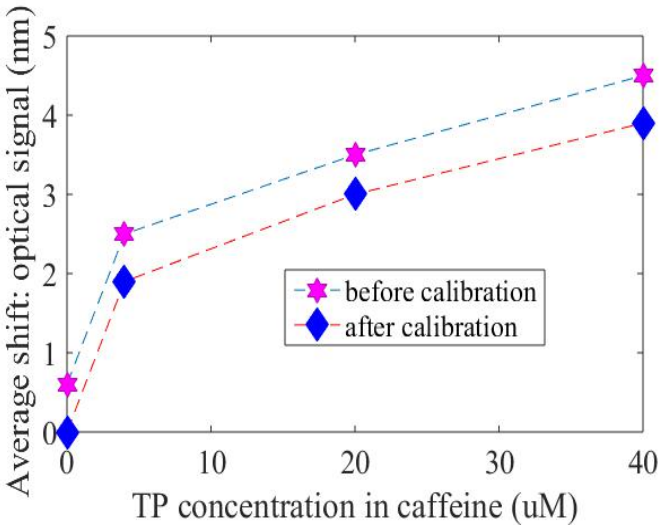

Figure 7.Optical response: Fringes shift for different concentration of theophylline (TP) in caffeine before and after the calibration

The optical signals for theophylline in caffeine is given in **Fig. 7**. As shown, even without theophylline in caffeine, the shift is ~0.5 nm, again indicating the small non-specific binding exists between the aptamer and caffeine as expected. Using the shift with only caffeine as a reference, the calibrated curve can be obtained as shown in **Fig. 7**.

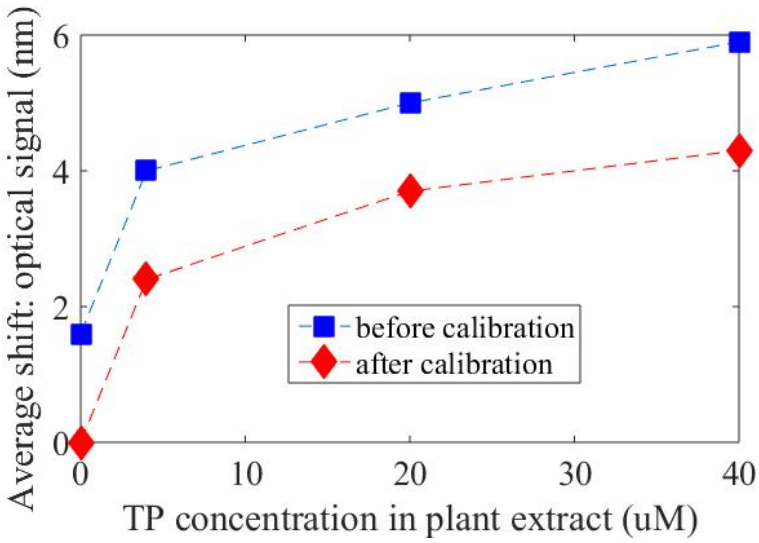

Figure 8. Optical response: Fringe shift for different concentration of theophylline

(TP) in plant extract with MeOH before and after the calibration.

Finally, the measurements of theophylline dissolved in plant extract are given in **Fig. 8**. As shown, some levels of the non-specific binding between aptamer with plant extract exist. Nevertheless the calibrated measurement indicates the sensor can detect theophylline in plant extract successfully.

References

[1] P.J.BarnesandR.A.Pauwels,"Theophylline in the management of asthma: time for reappraisal?" Eur.Respir.J.,1994,vol.7,pp.579–591,1994.

[2] A.H. DawsonandI.M.Whyte,"Therapeutic drug monitoringin drug overdose," Br.J. Clin.Pharmacol.,vol.48,pp:278–283,1999.

[3] C.E. Cook,M. E.Twine,M. Myers,E. Amerson,J. A. Keplerand G. F.Taylor, "Theophylline radioimmunoassay: synthesis of antigen and characterization of antiserum," Res.Commun.Chem.Pathol.Pharmacol.,vol.13,pp:497–505,1976.

[4] B.Srdjenovic,V.Djordjevic-Milic,N.Grujic,R.InjacandZ.Lepojevic, "Simultaneous HPLC Determination of Caffeine, Theobromine, and Theophyllinein Food, Drinks, and Herbal Products,"J.Chromatogr.Sci., vol.46,pp:144–149,2008.

[5] M.E.Jolley,"Fluorescence polarization immunoassay for determination of the rapeutic drug levels in human plasma,"J.Anal.Toxicol.,vol.5,pp: 236–240,1981.

[6] E.E.Ferapontova, E.M.OlsenandK.V.Gothelf, "AnRNAaptamer- based electrochemical biosensor for detection of the theophylline in serum," J.Am.Chem.Soc.,vol.130,pp:4256–4258,2008.

[7] Y.V.Ulyanova, A.E.Blackwell and S.D.Minteer,Analyst, "Poly(methylenegreen) employed

as molecularly imprinted polymer matrix for electrochemical sensing," vol.131, pp:257–261,2006.

[8] K.Song,S.Lee,and C.Ban." Aptamers and their biological applications." Sensors, vol.12,no.1, pp:612-631,2012.

[9] H.Yin,X.Li,andL.Que."Fabrication and characterization of aluminum oxide thin film micropatterns on the glass substrate."Microelectronic Engineering, vol.128, pp:66-70,2014.

[10] S. Alzghoul, M.Hailat,S. Zivanovic,L. Que,G.Shah," Measurement of serum prostate cancer biomarker susinga nanopore thin film based optical of fluidic chip," Biosensors and Bioelectronics,77,pp:491-498,2016.

[11] T.Zhang,Y.He, J.Weiand L.Que, "Nanostructured optical microchips for cancer biomarker detection,"Biosensors and Bioelectronics, 38,pp: 382-388,2012.

CHAPTER 3. ADDITIONAL WORK RELATED TO RAPID DETECTION OF THEOPHYLLINE USING AN APTAMER-BASED NANOPORE THIN FILM SENSOR

Abstract

This reports describes additional work related to an aptamer-based nanopore thin film sensor for detecting theophylline in different concentrations and testing the influence of theophylline in serum. It alsodescribes determination of binding kinetics for duration times ranging from 1 minute to 2 hours to find the fit incubation time. The experiments found that an aptamer-based sensor can detect theophylline at concentrations as low as 0.2 μM and as high as 48 μM and also that an aptamer-based sensor can detect theophylline in serum..

Introduction

The first experiment was to test the theophylline dynamic range achieved in using anaptamer-based sensor. First the different concentrations of theophylline were tested, then all the shifts and averages for each concentration were calculated. The process requires adding a theophylline solution to the sensor followed by incubation for 2 hours. Since we wanted to see whether a 2 hourreaction time was necessary, twe wanted to determine the binding kinetics. Since the final goal was to use an aptamer-based sensor to detect the concentration in serum, the last experiment involved detection of the theophylline dissolved directly in Newborn Calf Serum.

Assess theophylline sensitivity and dynamic range

In this experiment, the concentration of theophylline for 0.2μM, 1μM, 2μM, 4μM, 8μM,

16μM, 32μM and 48μM was tested, with eachtest repeated 5 times. Table 1 shows the average shift of the fringes at each concentration. As expected, the higher the concentration of theophylline, the larger the shift of the fringes, as shown in **Figure 9**.

Table 1. Average fringe shifts for each concentration of theophylline

Concentration(μM)	0.2	1	2	4	8	16	32	48
Average shift	0.553	2.233	2.548	3.448	3.536	3.695	4.253	4.457

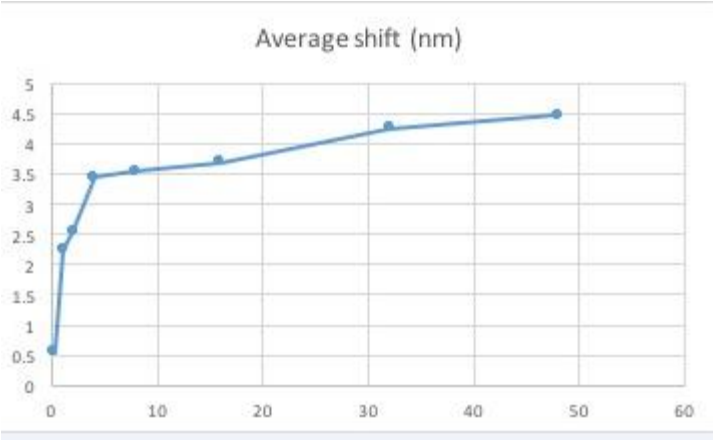

Figure 9. Plot for average fringe shifts VS Concentration of theophylline

Table 1 shows that in 0.2μM theophylline, the shift is about 0.553. Experiments found that the aptamer-based sensor, without any optimization, can detect theophylline at a concentration as low as 0.2μM, a level comparable to the detection limit of current lab-based procedures such as liquid chromatography (LC). Note that the detection limit of the sensor can be further improved by modifying the nanopore size and density.

Figure 9 clearly shows that, as the concentration increases, the shifts become larger.

Determination of Binding Kinetics

The process is described in Chapter 2 with specific details given in Appendix A. The last step is adding the theophylline solution on the aptamer-based sensor followed by an incubation of 2 hours ensure that make sure the reaction is complete. To shorten the incubation time, 48μM of theophylline was used to test the duration. The tested binding duration times were 1,2,10,15,30,60,and 120 minutes. More specifically, after each duration time, a PB buffer was used to rinse the aptamer-based sensor, followed by waiting for it to dry and then test the fringes shift. **Figure 10** shows the fringes shift values recorded. **Table 2** shows the number of shifts for each duration time, and **Figure 11 is** a graph showing the trend. As can be seen in **Figure 11**, after 1 hour the shift becomes saturated, indicating that the reaction was totally finished after about 1 hour, so the duration time can be reduced from 2 hours to 1 hour.

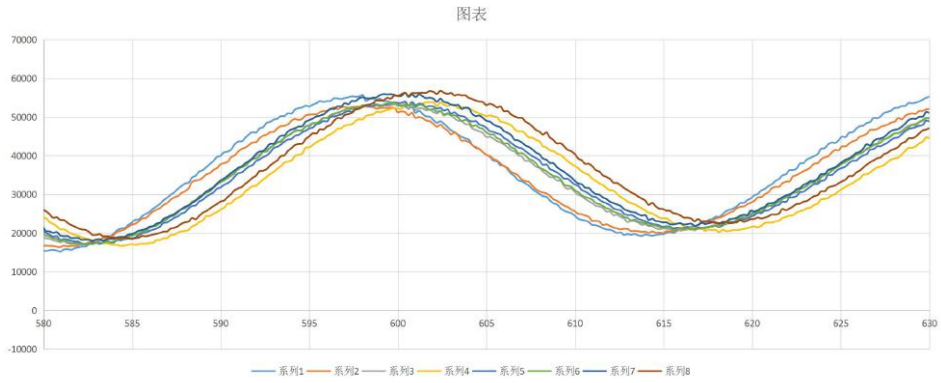

Figure 10**. Fringes at each duration time**

Table 2. Fringe shifts in each duration time

Duration time (mins)	1	2	10	30	60	120
Shifts (nm)	1.001333	1.398	2.397	2.5296667	3.1943333	3.3946667

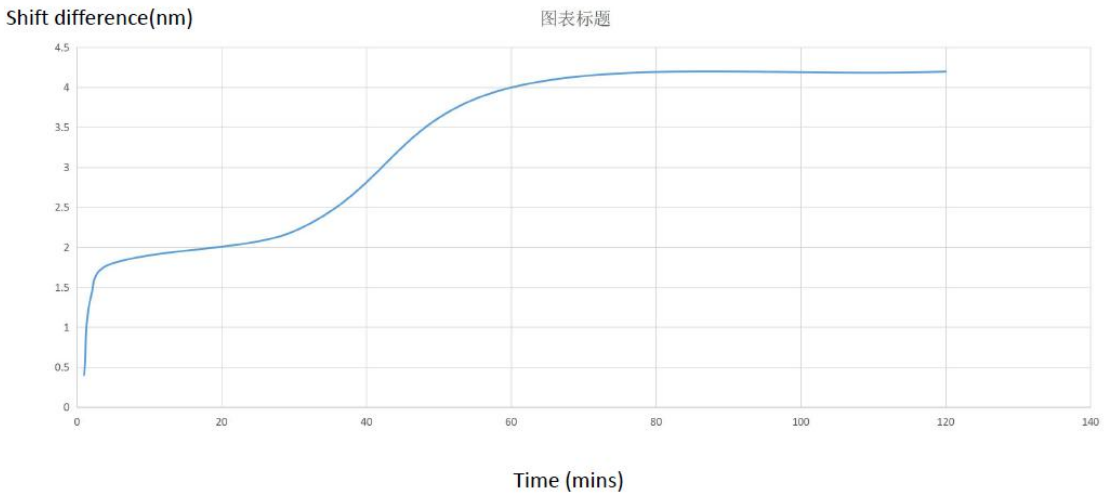

Figure 11**. Duration time VS Fringe shift.**

Test Influence of Serum

After successful detection of the theophylline in caffeine, theobromine, and plant extract an attempt to detect the theophylline dissolved in serum was made. The experiment involved detection oflevels of 0μM, 4μM, and 40μM theophylline dissolved in Newborn Calf Serum(NBCS). The reason for choosing Newborn Calf Serum was that newborn calf serum collected from calves typically 20 days old or younger are processed and manufactured in New Zealand, and each lot of newborn calf serum is tested for its ability to support the growth of VERO cells over three subcultures. At each passage, the cells sub cultured to the original cell-inoculation density [1]. However, even thoughNewborn Calf Serum contains a complex array of protein components required by many cells to grow, unfortunately large quantities of undefined proteins can lead to undesired stimulation of cells [2].To avoid such other proteins affecting the result of the experiment, after the reaction the apatamer-based sensor was rinsed five times.**Figure 12**through**Figure 14** show the fringe shift for 0μM, 4μM, and 40μM

theophylline dissolved in Newborn Calf Serum.

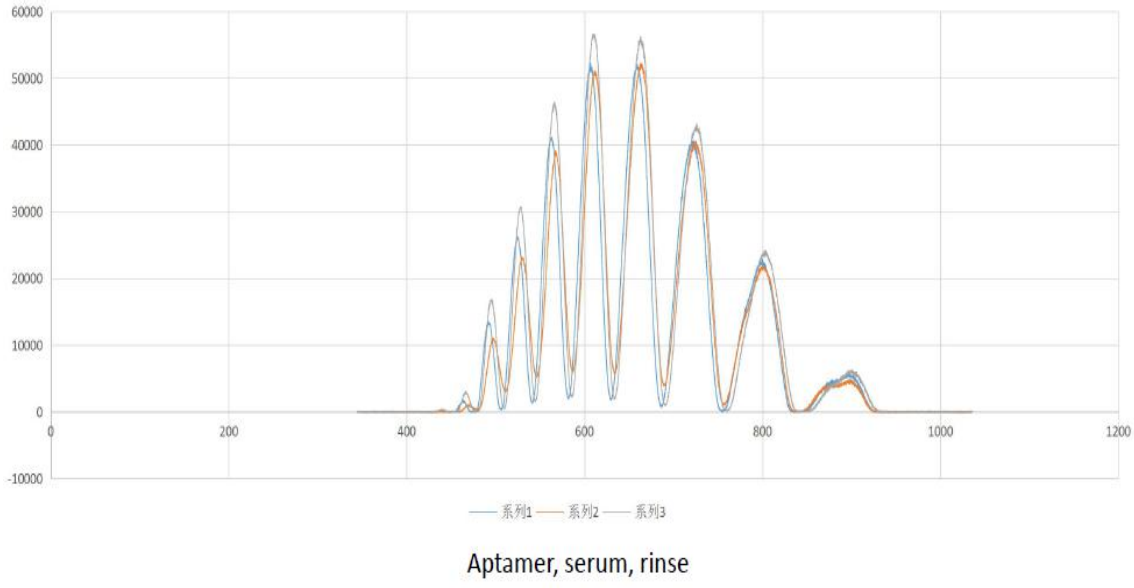

Figure 12**. 0µM theophylline dissolved in NBSC. Compared by aptamer, serum and after rinse**

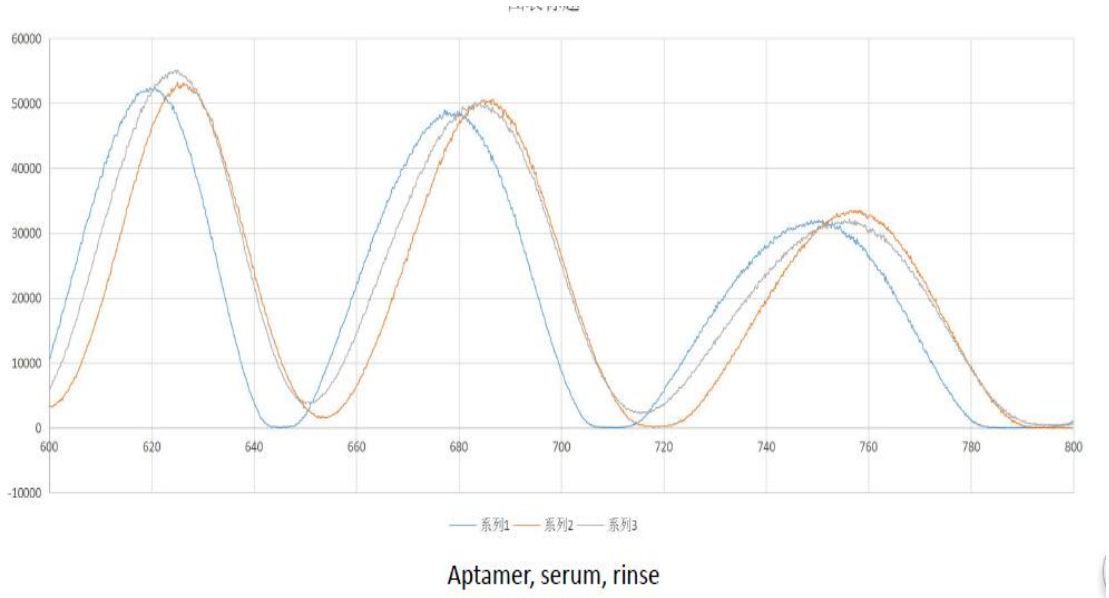

Figure 13**. 4µM theophylline dissolved in NBSC. Compared by aptamer, serum and after rinse**

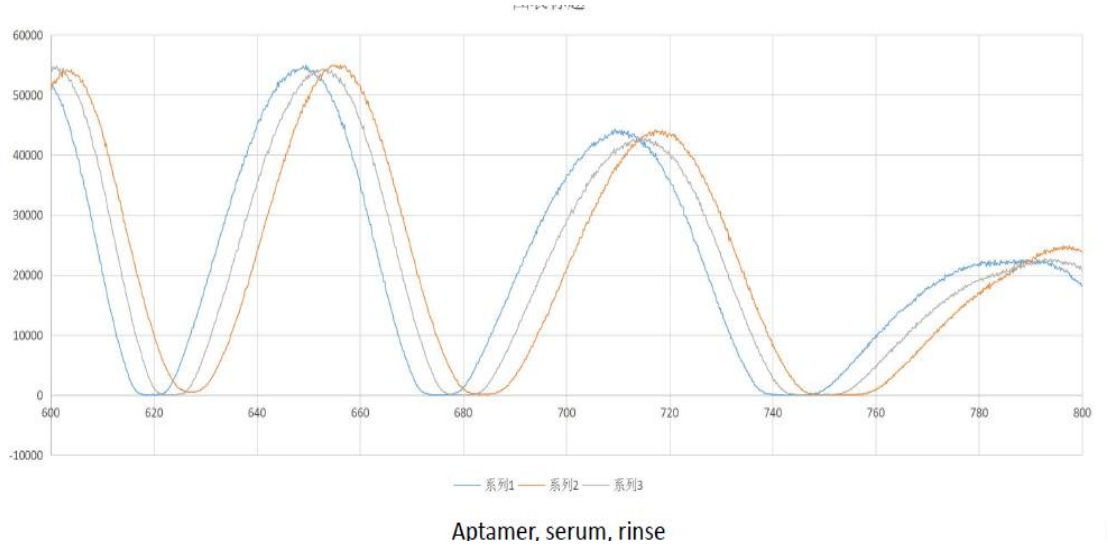

Figure 14**. 40µM theophylline dissolved in NBSC. Compared by aptamer, serum and after rinse**

Figure 12shows that, after the rinse, the fringes are close to those of the fringe for aptamer, meaning that if no theophylline is found in in the NBSC, the aptamer-based sensor cannot detect anything. Comparing **Figures 13 and 14** shows that the fringes are obviously shifted. This experiment demonstrates that an aptamer-based sensor can detect only the theophylline with high selectivity. These measurements were followed by calculating results for the average values **(Table 3)**. According to the data from Table 3,the shift between 4µM and 40µMhad a very small small difference. Since NBSC consists of many different proteins and impurities that can affect the results of the experiments, the aptamer-based sensor's specificity was reduced.

Table 3. Shift with different theophylline concentration dissolved in NBSC

Concentration (µM)	0	4	40
Shift (nm)	0.8	4.277	4.395333333

To solve this problem, the experiments for 4µM and 40µM theophylline dissolved in

NBSC were redone, this time using Newborn Calf Serum diluted 20 times by PBS buffer to reduce impurities. The resulting shifts are shown in **Table 4**. Comparing the data from Table 3 and Table 4 shows that, after dilution in NBSC, the shift became smaller, indicating reduction in impurity level. The difference in shift between 4μM and 40μM theophylline increased from 0.1183nm to 0.21107nm.

Table 4. Shift with different theophylline concentration dissolved in NBSC that diluted 20 times by PBS buffer

Concentration (μM)	4	40
Shift (nm)	3.0396	3.250666667

However, the shift difference is still very small, perhaps because using different types of AAO led to a thickness change in AAO. Since the aptamer-based sensor selectivity is due to the AAO thickness, using a different AAO thickness would result in different selectivity.

To determine whether thickness is the reason for this problem, two control experiments were designed. The first experiment used the same AAO thickness to test both 40 μM theophylline solution and 40 μM theophylline dissolved in serum. The second experiment used different thicknesses of AAO to test 40 μM theophylline dissolved in serum. Comparing both fringe shift from both experiments should make it easy to determine the main source of the problem.

References

[1] "Newborn Calf Serum" Thermo Fisher Scientific.Web. https://www. thermofisher.com/us/en/home/life-science/cell-culture/mammalian-cell-culture/fbs/ other-sera/newborn-calf-serum.html

[2] "Fetal bovine serum" Wikipedia.Web. https://en.wikipedia. org/wiki/ Fetal_ bovine_ serum#Technical_issues

CHAPTER 4. DETECTION OF PLANT HORMONE ABSCISIC ACID (ABA) USING AN OPTICAL APTAMER-BASED SENSOR WITH A MICROFLUIDICS CAPILLARY INTERFACE

Modified from an abstract to be submitted to MEMS-Biosensors and Bioreactors

Chao Song, Xiangchen Che, Silu Feng, Long Que

Abstract

This paper reports for the first time an optical aptamber-based plant hormone sensor with a microfluidics capillary interface. The ssDNA aptamer-based sensor has sensitivity with excellent specificity for detecting abscisic acid (ABA) superior to that of the ELISA detection kit from Sigma, reflecting its potential for screening different plant hormones in a complicated matrix. Its microfluidics capillary interface also allows samples to be automatically delivered to the sensor without use of external pumps, paving the way for point-of-care application in the field.

Instruction

Most physiological and development processes in plants are regulated by plant hormones, small molecular natural products including auxins, cytokinins, gibberellins (GA), abscisic acid (ABA), ethylene, etc. [1]. It is important to quantitatively analyze plant hormones for in-depth study of their biosynthesis, transport, metabolism and molecular regulatory mechanisms. Current widely-used laboratory procedures for detecting plant hormones include radioimmunoassay, enzymelinked immunosorbent assay (ELISA), chromatography, and chromatography/mass spectrometry [1-3]. These methods usually require skilled personnel and long-time analysis at high cost, hence are not suitable for point-of-care (POC) testing in

the field. Electrochemical techniques represent an alternative approach promising simplicity, convenience and low cost [1], but poor stability and reproducibility are hurdles to their wide application in practice. Presently, electrochemical biosensors remain at an early stage of methodology for detecting plant hormones.

For this experiment, the main differences from procedures of Chapter 2 arethe design of a microfluidics capillary interface allowing samples to be delivered to the sensor, and testing the plant hormone abscisic acid(ABA).

This chapter will introduce what the microfluidics capillary interface, the mask schematic, and the fabrication process.

Microfluidics Capillary Interface

Microfluidic devices are promising for applications that require precise displacement of small amounts of liquids or that can benefit from peculiar behaviors that liquids and chemical reactions exhibit at micrometer length scale [4]. A microsystem is typically composed of three major components: impedance microsensors, open-channel capillary micropumps, and passive microfluidic stop-valves [5].

In our device, we focused on capillary micropumps and passive microfluidic stop-valves. Capillary pumps are comprised of microstructures of various shape with dimensions from 15-250 μM, and positioned in the capillary pumps to encode a desired capillary pressure. The capillary pumps are designed to have a small flow resistance and are preceded by a constricted microchannel that acts as a flow resistance [6]. The passive stop-valve array prevents the liquid from getting into an undesired part of the platform because of a sharp change in the liquid-sidewall angle [5].

As will be shown below, a flow resistance in front of the capillary pump can also be used

in capillary pumps to modulate the filling behavior of liquids. The flow rate Q of a liquid in a CS is determined by the wettability of the CS, the viscosity of the liquid, the total flow resistance, and the capillary pressure in the capillary pump, and can be expressed as

$$Q = \frac{1}{\eta}\frac{\Delta P}{R_F} \tag{1}$$

where η is the viscosity of the liquid, the difference in pressure inside and in front of the liquid. the total resistance to flow of the flow path, a microchannel of variable length dominates the flow resistance. The resulting pressure of a liquid-air meniscus in such a rectangular microchannel is

$$P_C = -\gamma\left(\frac{\cos\alpha_b + \cos\alpha_t}{a} + \frac{\cos\alpha_l + \cos\alpha_r}{b}\right) \tag{2}$$

where is the surface tension of the liquid, are the contact angles of the liquid on the bottom, top, left, and right wall, respectively, and a and b are the depth and width of the microchannel, respectively [6]. The flow resistance of such microchannels is a geometric term expressed as a Fourier series and can be approximated by a linear term [7].

$$R_F = \left[\frac{1}{12}\left(1 + \frac{5}{6}\frac{a}{b}\right)\frac{abR_H^2}{L}\right]^{-1} \tag{3}$$

satisfying the condition, a, b. Here L is the length of the microchannel and is the hydraulic radius of the microchannel,

$$R_H = \frac{2A}{P} = \frac{ab}{a+b} \tag{4}$$

with P being the perimeter and A the area of the cross section of the microchannel. The flow in a microchannel can thus be estimated using the capillary pressure divided by the flow resistance that continually increases as the channel is being filled [6].

Microfluidics capillary fluidic chip design

Mask design is the first step in designing a microfluidics capillary fluidic chip,. I used L-edit and Auto-CAD to draw the layout. These two familiar software tools are commonly used for layout, with L-edit often used for transistor design.

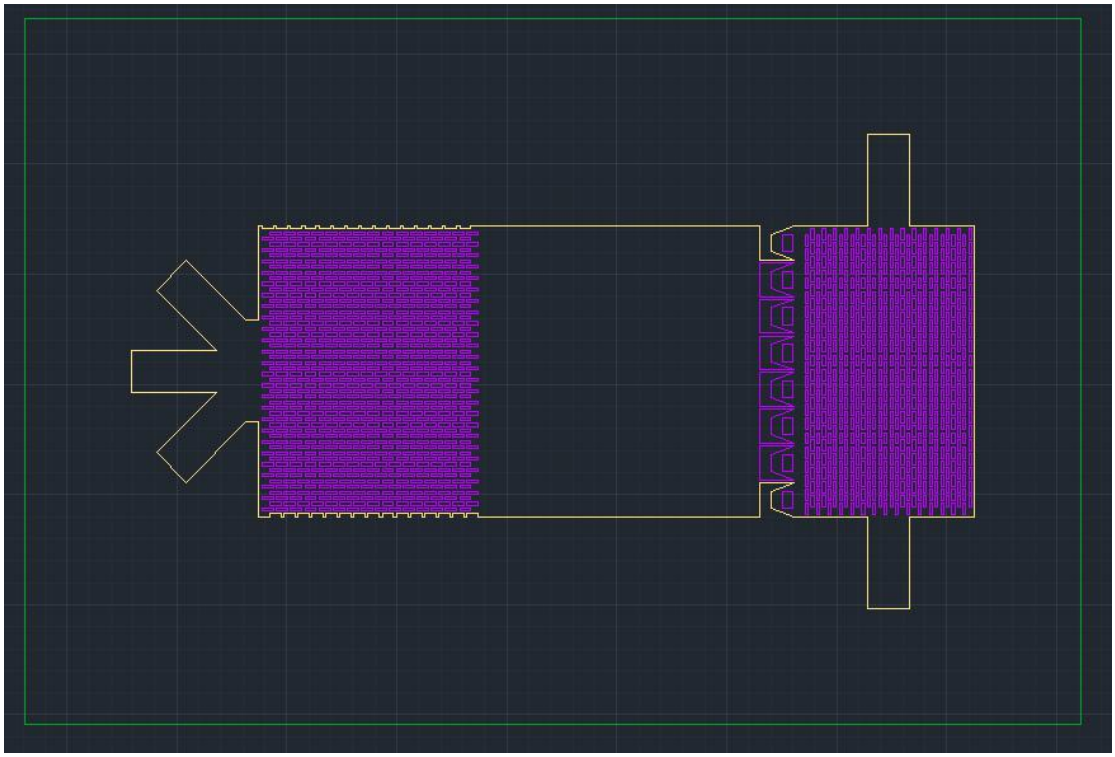

Figure 15**. Layout for microfluidics capillary fluidic chip by Auto-CAD**

The microfluidics chip consists of six main parts: pillar, pump, stop-valve, space for AAO, input, and output. Each pump consists of arrays of pillars. As shown in **Figures 15** and **Figure 16**, once the solution passes into the chip at input 1, it would cross pump 1 slowly to reach the space where the AAO is located. After the solution passes through the AAO space , it reaches to the stop-valve where it is stopped and lo longer flows. After the reaction between solution and AAO is finished, I a solution is introduced into input 2 to rinse the chip, after which the fluid would go through to the pump 2. At this time, since the pressure in pump2 and the stop-valve become equal, the solution stopped at the stop-valve would go through to pump2.

Finally, all the fluids would flow out. Three inputs were used because several different solutions had to be added.

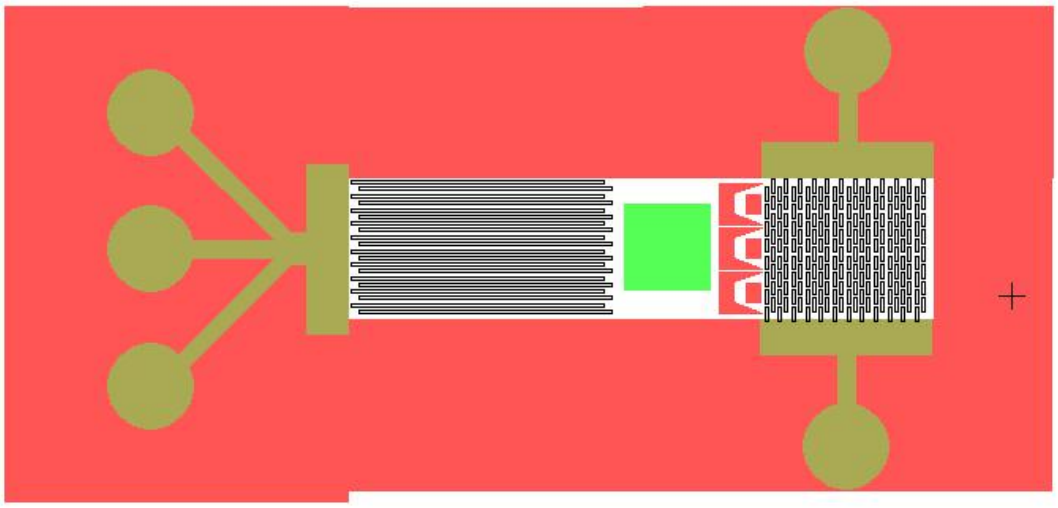

Figure 16**. Layout for Microfluidics capillary chip by L-edit**

To ensure that the mask would work properly, 4 different size of pillars were included. The mask should be designed to fit on a 1 inch * 3-inch wafer. **Figure 17** shows the shapes and size of the pillars for mask 1 through mask 4. F**igures 18** through **20** show the the detailed schematic for mask 1; the other three masks are similar to and their schematics are shown in Appendix B. Pump 1 consisted of fifteen repeated arrays of fifteen pillars. The space between the two arrays is 200 μm, shown for pump1 in Figure 4. Pump 2 is quite similar to pump 1. Pump 2 used 20 pillars repeated in 30 arrays as shown in **Figure 19**. Finally, the stop-valve was designed; 8 repeated stop-valve unit are shown in **Figure 20**. Total area of the AAO is 20000 * 20600 μm. The actual version is shown in **Figure 21**.

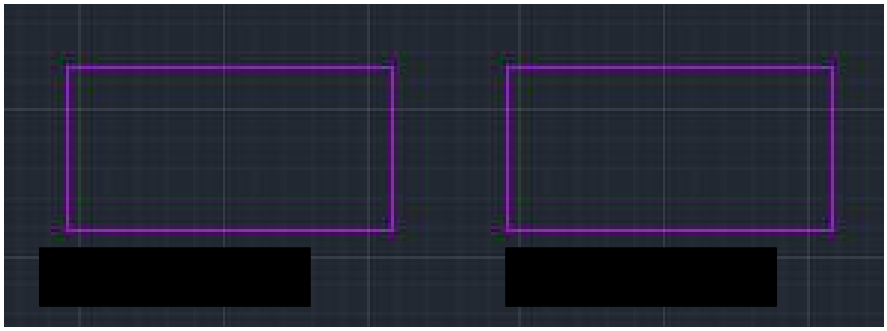

(a)Pillar size for Mask 1 **(b) Pillar size for Mask 3**

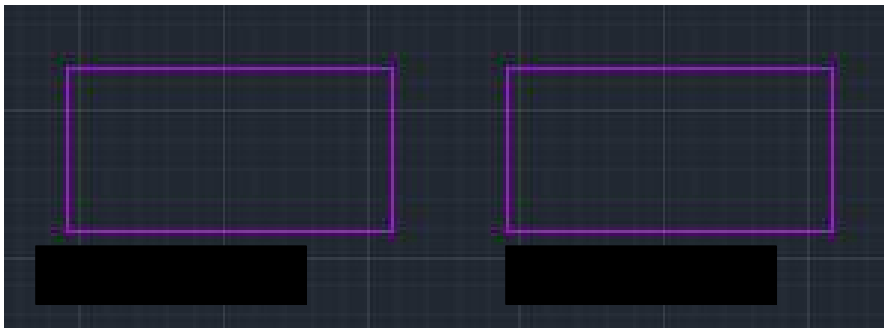

(c)Pillar size for mask 2 **(d) Pillar size for mask 4**

Figure 17**. Pillar's shape**

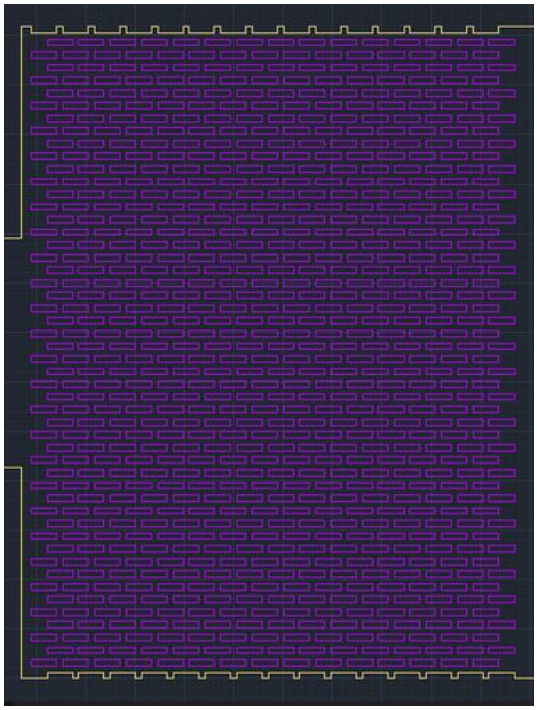

Figure 18**. Pump1**

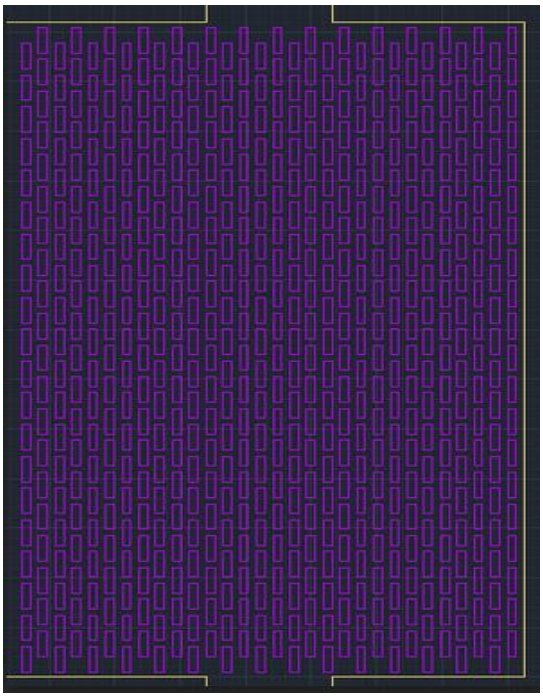

Figure 19**. Pump 2**

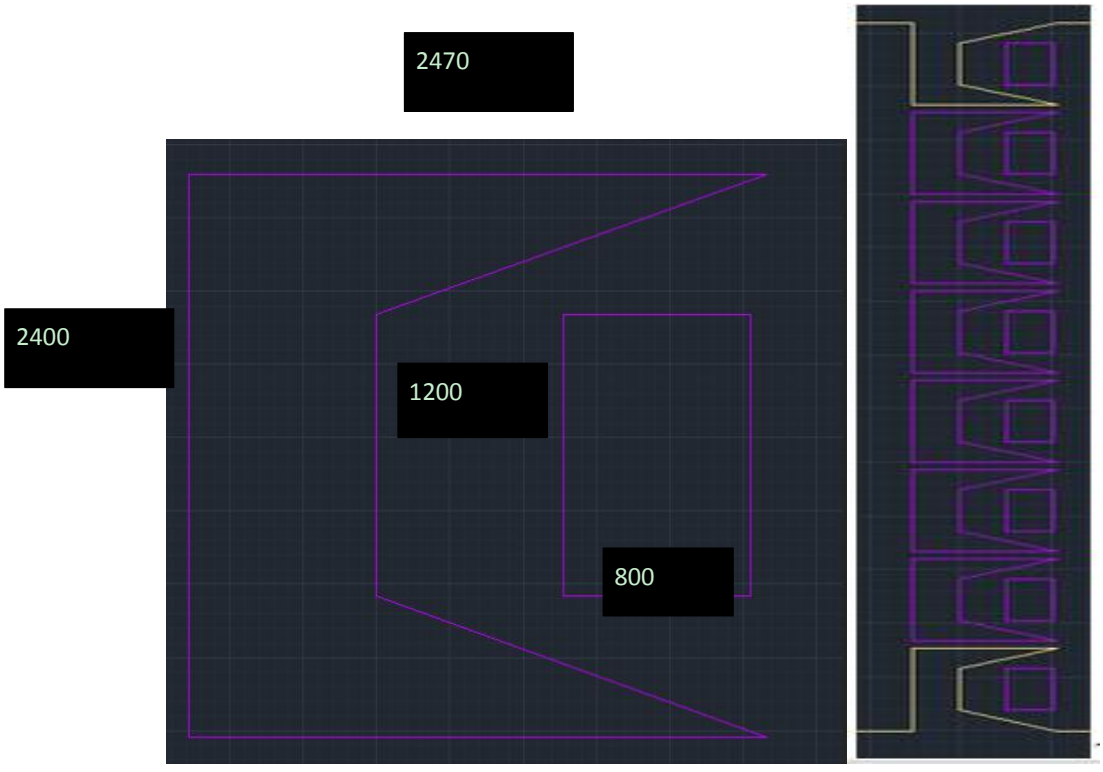

(b)

Figure 20**. (a) the shape and size for unit stop-valve. (b) the array of stop-valve.**

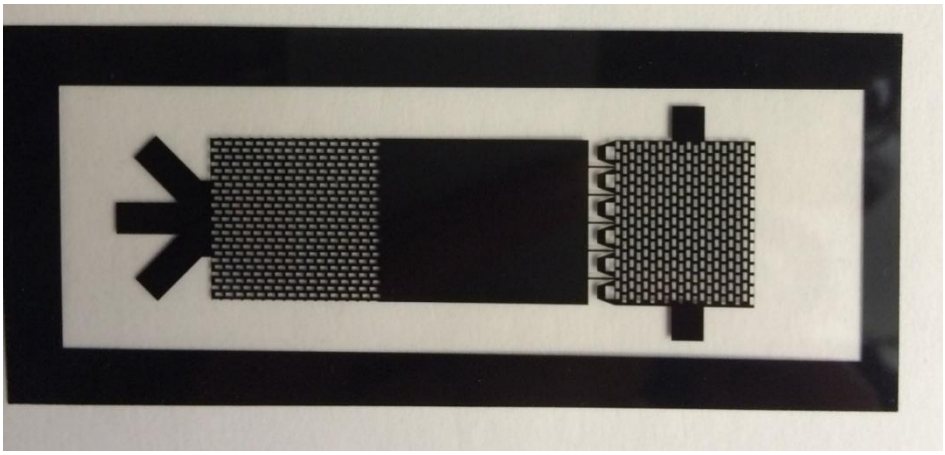

Figure 21**.Actual Mask.**

Microfabrication

Themicrofluidics capillary chips were fabricated in AAO using photolithography and etching. The fabrication process is comprised of the five main steps shown in **Figure 22**. They are: a) E-beam Al deposition (100nm); b) AZ-5214 positive photoresist as protection layer; c) Photolithography and Al/AAO etching to form the AAO pattern; d) SU-8 negative photoresist apply; e) Photolithography to form the final SU-8 pattern.

Aluminum Etching

To etch aluminum, there must be a mask covering the aluminum plane photoresist. Az was used as the mask because it is very easy to use photolithographic processes to make an Az mask and that mask can be rinsed in acetone after etching aluminum. The detailed process is:

1. Clean the wafer prior to starting processing with IPA and Ethanol.

2. Put wafer in spinner, first drop HMDS and set spin speed to 4000 rmp for 20 seconds. After spreading out the HMDS, drop Az to cover whole aluminum area and set speed to 4000 rmp for 45 seconds. Spin to speed out Az to obtain a 1.2um thickness Az plane.

3. Pre-bake the wafer at 95° C for 1 minute.

4. Place the mask over the Az plane and expose the wafer to UV light at 10 intensity for 20 seconds.

5. Postbake the wafer at 120° C for 2 minutes.

6. Pour some Az developer into a glass dish. Place the wafer in the developer and gently agitate the developer for about 60 seconds.

7. Clean the Az developer with water.

8. Pour some Aluminum Etchant Type A into a glass dish. Place the wafer in the developer and gently agitate the developer for about 1 hour.

9. Rinse the Az mask with acetone 10. Bake the wafer at 85° C to dry the surface.

While etching aluminum, we must be very careful about exposure and development time. If exposure time is too short, the masked features will come off during development, and similarly, if the development time is too long, the feature will also come off.

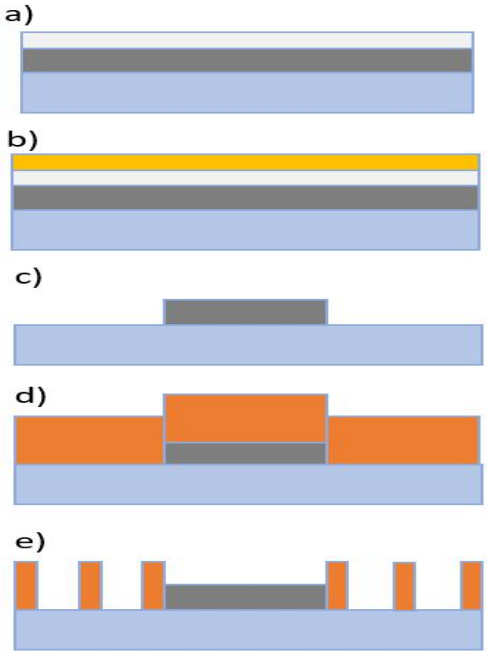

Figure 22. Fabrication process

SU-8 Spin-coating & Photolithography

SU-8 is a commonly used epoxy-based negative photoresist. A negative photoresist is one

for which the parts exposed to UV become cross-linked while the remainder of the film remains soluble and can be washed away during development. (2) The process of spin-coating is followed by using the following standard instructions:

1. Wash the silicon wafer using DI water and ethanol. Then use an air gun to dry it, and oven-bake at 100 degrees for 3 minutes.

2. Spin the SU-8 on the silicon with rotation speed of 1100rpm/s.

3. Pre-bake the wafer at 65 degree, increase the temperature at the rate of 10 degree per 10 minutes to 95 degrees, and bake for 90 minutes.

4. Put the mask on the silicon wafer and expose with the UV central intensity set at 10mW/ for 60 seconds.

5. Post-bake (or soft bake) at 65 degrees for 12 minutes, increase the temperature at a rate of 10 degree per 3 minutes to 95 degrees, then bake for15 minutes.

6. Use SU-8 developer to develop the wafer for 15 minutes.

7. Wash with by IPA to see if there is any white floccule in the cube. If nothing is seen, the un-illuminated part has been totally removed.

8. Rinse the wafer using ethanol and DI water, then use anair gun to dry it.

9. Bake the wafer at 85 degrees for 6 minutes to keep the surface dry.

PDMS molding and bonding

PDMS is a highly viscous flowing liquid that helps form internal cross links that turn the PDMS into a flexible solid.

The process is as follows:

1. Pour the PDMS base (Sylgard 184 silicone elastomer base) followed by curing agent (Elastomer curing agent), with the base weight at 10 times the curing agent weight.

2. Mix for about 5 minutes making sure that the curing agent is uniformly distributed.

3. If air bubbles are observed, place the container in a degasser for about 1 hour to allow the trapped air bubbles to escape. .

4. Spin about 5 g of the PDMS over the molds to ensure that the thickness of about 2mm. Allow the PDMS to flow and form a blob atop the mold. Spinning will even this out, with moderate edge bead effects, leaving a thin layer of PDMS on the SU-8 molds underneath.

5. Post-bake at 150 degrees for 6 mins.

6. Wait for the PDMS to cool, then use a sharp holder to tweak around the edges and peel the PDMS.

7. Bond the PDMS and substrate together in an Oxygen Plasma machine using the following standard procedure:

- Load the sample inside the plasma machine chamber
- Use a vacuum pump to pump out air from the machine's chamber.
- Fill the chamber with oxygen at a regulated pressure of 8 psi and begin stable between 0.2~0.4 mbarr point in flow meter on the plasma machine for 20 seconds.
- Open plasma generator for 10 s.
- Ventilate the chamber, unload the sample, and bond samples.

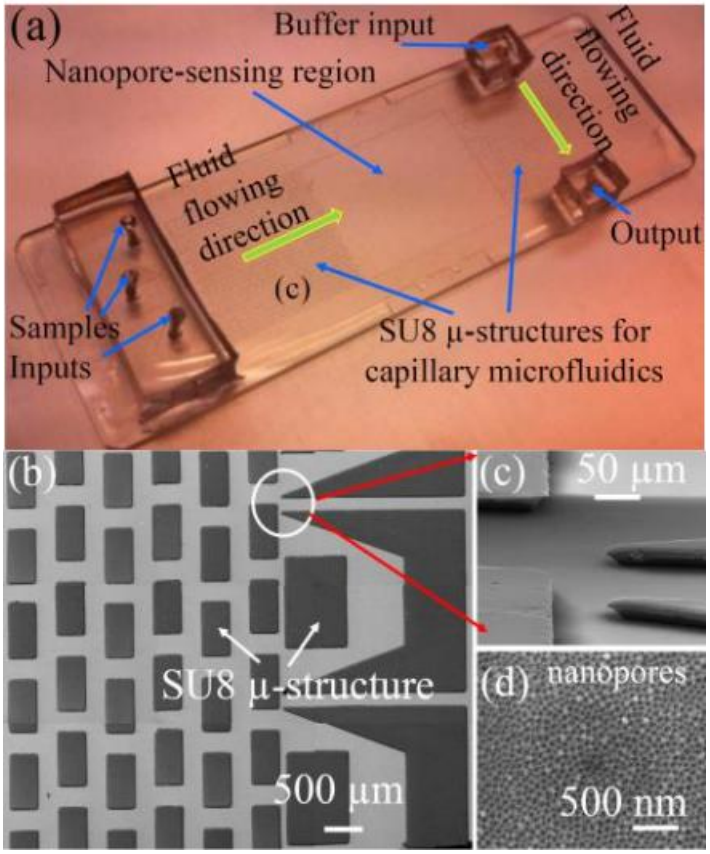

Figure 23 (a) Photo of a fabricated chip bonded with PDMS slabs with inputs and outputs; (b-d) SEM images of the SU8 microstructures for capillary microfluidics and the nanopore-sensing region fabricated from anodic aluminum oxide (AAO).

A sensor chip photo is shown in **Figure 23a**. Optical micrographs and SEM images of the SU 8-based microfluidics capillary structures and nanopore-sensing elements are shown in **Figures 23b-d**.

References

[1] Fu, J., Sun, X., Wang, J., Chu, J., & Yan, C. "Progress in quantitative analysis of plant hormones"Chinese Science Bulletin, 2011, 56(4-5), 355-366.

[2] Müller M., Munné-Bosch S. "Rapid and sensitive hormonal profiling of complex plant samples by liquid chromatography coupled to electrospray ionization tandem mass spectrometry". Plant Methods 2011, 7(1), 1-11.

[3] Pan, X., Welti, R., & Wang, X "Quantitative analysis of major plant hormones in crude plant extracts by high-performance liquid chromatography–mass spectrometry". Nature Protocols, 2010, 5(6), 986-992.

[4] J. Ducrée and R. Zengerde, "Microfluidics", Springer, Berlin , 2006.

[5] F. Zang, K Gerasopoulos, K. McKinzie, J.N.Culver and R. Ghodssi, "Autonomous capillary microfluidics for rapid nanoreceptor assembly and biosensing", IEEE, 2015.

[6] Martin Zimmermann, Heinz Schmid, Patrick Hunziker and Emmanuel Delamarhe. "Capillary pumps for autonomous capillary systems", The royal Society of Chemistry 2007.

[7] J.H.Spurk, in *Strömungslehre*, Springer, Berlin, 2004, pp. 164-167.

CHAPTER 5. GENERAL CONCLUSIONS

General Discussion

Chapter 2 and Chapter 3 have assessed theophylline sensitivity and dynamic range, determined binding kinetics, tested ligand specificity, and, finally, tested influence of serum and plant extracts. Experiments have shown that a theophylline concentration of t 0.2 μM can be readily detected by an aptamer-based sensor. Experiments have also demonstrated good specificity and selectivity for aptamer-based sensors. Using nanopore thin film sensors, the experiment found that the fringes shift is ~0.2 nm when only caffeine, theobromine, and plant extract is applied, and, conversely, the fringes shift is much greater when theophylline is added to those solutions. This experiments reports for the first time successful use of an aptamer-based nanopore thin film sensor for detecting theophylline in buffer and complex fluids.

The study of Chapter 4 was very similar in style and analysis to that of Chapter 2. The former study attempted to use an optical aptamer-based plant hormone sensor with a microfluidics capillary interface to detect abscisic acid (ABA). My main experimental role in this study was to design and fabricate a microfluidics capillary chip whose microfluidics capillary interface allowed samples to be automatically delivered to the sensor without external pumps, paving the way for point-of-use application in the field.

Recommendations for Future Research

One of the advantages described in Chapter 2 is low cost. The best way to reduce cost by the greatest amount is to reduce the concentration of aptamer, and this can be experimentally studied by successively reducing the concentration from 5μM to 1μM, 0.5μM,, etc., to find the limit of detection.

In my experiments, I already tested the concentration of theophylline in the range from 0.2 μM to 48 μM. This can be repeated to record additional data to attempt achievement of a standardized determination of fringes shift vs concentration of theophylline. In addition, as mentioned in Chapter 2, the nanopore size of our AAO is 30 nm to 50 nm, and the sensor's detection limit can be further improved by modifying the nanopore size and density and also increasing the thickness.

Following this experiment, we can forsee much additional work. First, we can assess the influence of RNase inhibitor on assay. Small amounts of ribonucleases (RNases) can sometimes co-purify with isolated RNA and compromise downstream applications. Such contamination can also be introduced via tips, tubes, and other reagents used in various procedures. RNase inhibitors are commonly used as a precautionary measure in enzymatic manipulations of RNA to inhibit and control for such contaminants [1]. We choose SUPERase·In dissolved in PBS with 5 mM KCl and 1mM MgC. The test separates into two parts. The first test is for 0μM, 4μM, and 40μM theophylline dissolved in 0.1M PH7.2 PBS with 5 mM KCl and 1mM MgC. If it can clearly discern the fringe shifts, as the second experiment we will add the SUPERase·In into the solution and test again and then compare the two fringe shifts.

Finally, we can determine shelf life and the impact of storage buffer both with and without RNase inhibitor. For this experiment, we can use a sample like the one above after finishing the whole process for surface functionalization. We can put the sample incubator at 4 degrees over 0, 1, 2, 4, or 8 weeks.

References

[1] "RNase Inhibitors" Thermo Fisher Scientific.Web. https://www. thermofisher. com/us/en/home/life-science/dna-rna-purification-analysis/rna-extraction/rna-extraction-products/rnase-inhibitors.html

APPENDIX A. MATERIALS AND SURFACE FUNCTIONALIZATION

Materials

1.

• 0.1 mM 11-Mecaptoundecanoic acid ($HSC_{10}COOH$) and 0.9 mM 8-Mercapto-1-Octanol (HSC_8OH).

✓4.3672mg in 10ml absolute ethanol to get 2mM $HSC_{10}COOH$.

✓1ml 2mM $HSC_{10}COOH$ mix with 9ml absolute ethanol to get 0.2mM $HSC_{10}COOH$.

✓31.4ul HSC_8OH in 10ml absolute ethanol to get 18mM HSC_8OH.

✓1ml 18mM HSC_8OH, mix with 9ml absolute ethanol to get 1.8mM HSC_8OH.

✓mix 10ml 0.2mM $HSC_{10}COOH$ & 10ml 1.8mM HSC_8OH.

2. NHS and EDC

• 0.2M N-hydroxysuccinimide (NHS) and 0.05M N-(3-dimethylamnopropyl)-N-ethylcarbodiimide hydrochloride (EDC) in dH_2O o2.3018g NHS, 0.9585g EDC dissolve in 100ml dH_2O

3. 1M PH8 phosphate buffer

• 1M Na_2HPO_4: 56.784g Na_2HPO_4 dissolve in 400ml dH_2O

• 1M NaH_2PO_4: 11.998g NaH_2PO_4 dissolve in 100ml dH_2O

• 1M pH8 phosphate buffer: 372.8ml 1M Na_2HPO_4 + 27.2ml 1M NaH_2PO_4

4. ***Theophylline aptamer.*** [1]

• 5'-NH_2-$(CH_2)_6$-rAr GrUrGrArUrAr CrCrArGrCrArUr CrGrUrCr UrUrGrArUr GrCrCr CrUrUr GrGrCr ArGr CrArCrU (/5AmMC6/rArGrUr GrArUrAr CrCrAr GrCrAr Ur CrGr UrCrUrUr GrArUrGr CrCrCrUr UrGrGrCrArGrCrArCrU from IDT).

• Aptamers: theophylline = 1:2, Kd = 0.1 µM.

5. 0.1 M PH7.2 PBS with 5mM KCl and 1mM .

• 0.1481g KCl, 32g NaCl, 5.76g Na_2HPO_4, 0.96g KH_2PO_4, 0.08g $MgCl_2 \cdot 6H_2O$, dissolve in 400ml dH_2O, adjust pH using KOH.

6. 1M ethanolamine (EA) dissolved in dH_2O.

• 500µL EA dissolve in 9.401 ml dH_2O.

Surface Functionalization and Detection.

Figure 24 is the flow chart for surface functionalization, and the protocol is illustrated in **Figure 25**.

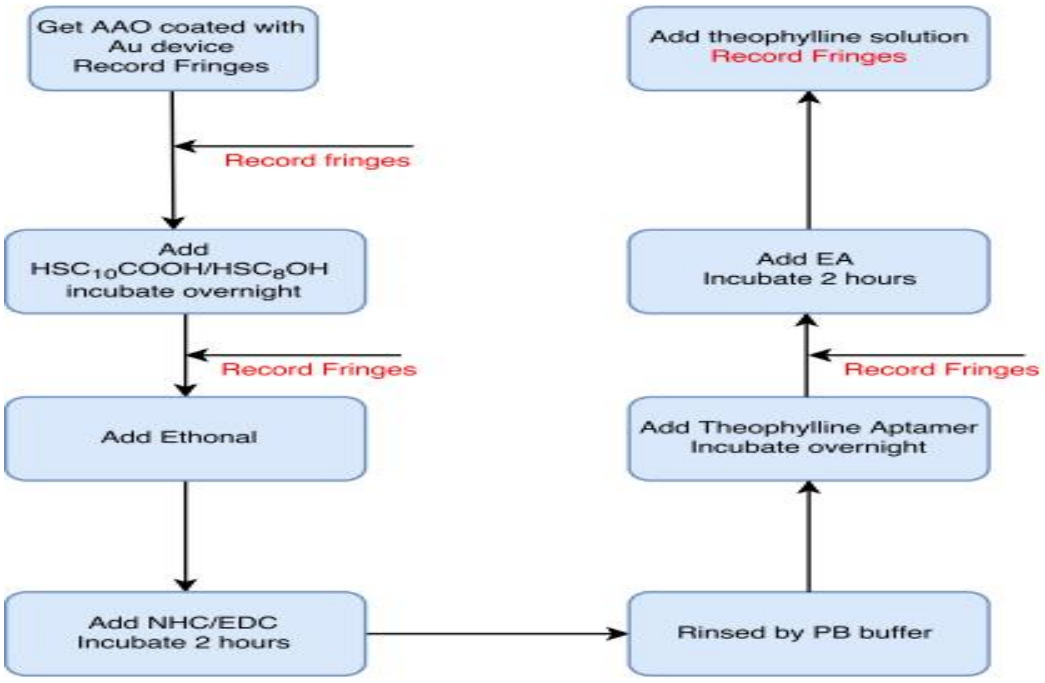

Figure 24.Flow chart for surface functionalization.

It is a well-established method to form a mixed SAM of alkanethiols by the adhesion reaction of the thiol group on a gold surface [1]. The monolayer is well packed and the tethered carboxylic acid is easy to functionalize for biological molecule immobilization [2]. When EDC/NHS is present, the carboxylic groups form active O-acylisourea intermediates, and readily react with primary amine groups that exist at the N-terminus of each polypeptide chain and in the side chain of lysine (Lys, K) residues. Because of their positive charge under physiologic conditions, primary amines are usually outward-facing of amptamer; hence, they are usually accessible for conjugation without denaturing ampater structure. In this way the aptamer active O-acylisourea intermediate groups are deactivated by the amino acid glycine to avoid non-specific biological attachment caused by the intermediates. At this stage, the aptamer are conjugated to the nanostructured surface and ready for theophylline detection [3].

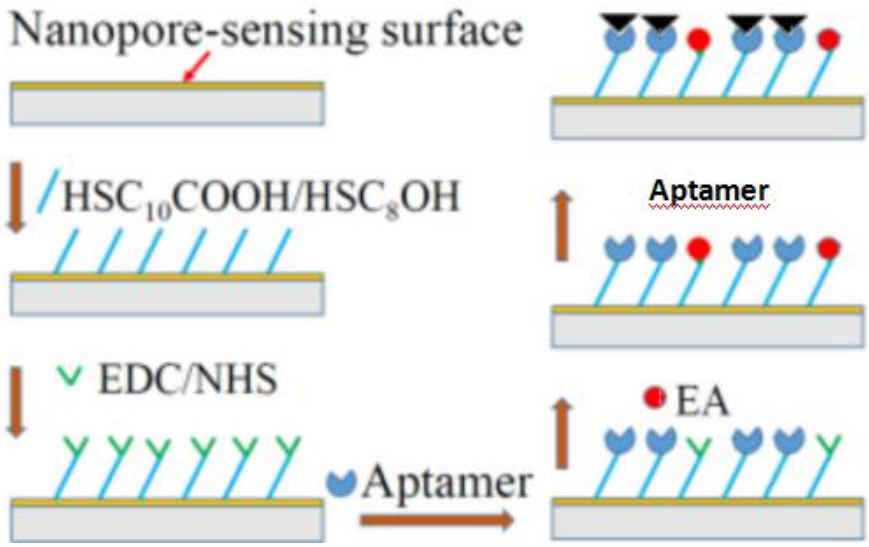

Figure 25.Surface functionalization procedure of the nanopore-sensing region for detecting theophylline using aptamer.

APPENDIX B. MASK SCHEMATICS

The Appendix B shows the other three schematic masks and also explain the meaning of each color.

The schematic of mask 2 is shows in **Figure26(a)-(d)**. For pump 1, each array has 16 pillars and there is a total of 32 arrays. For pump 2, each array has 20 pillars and there is a total of 20 arrays.

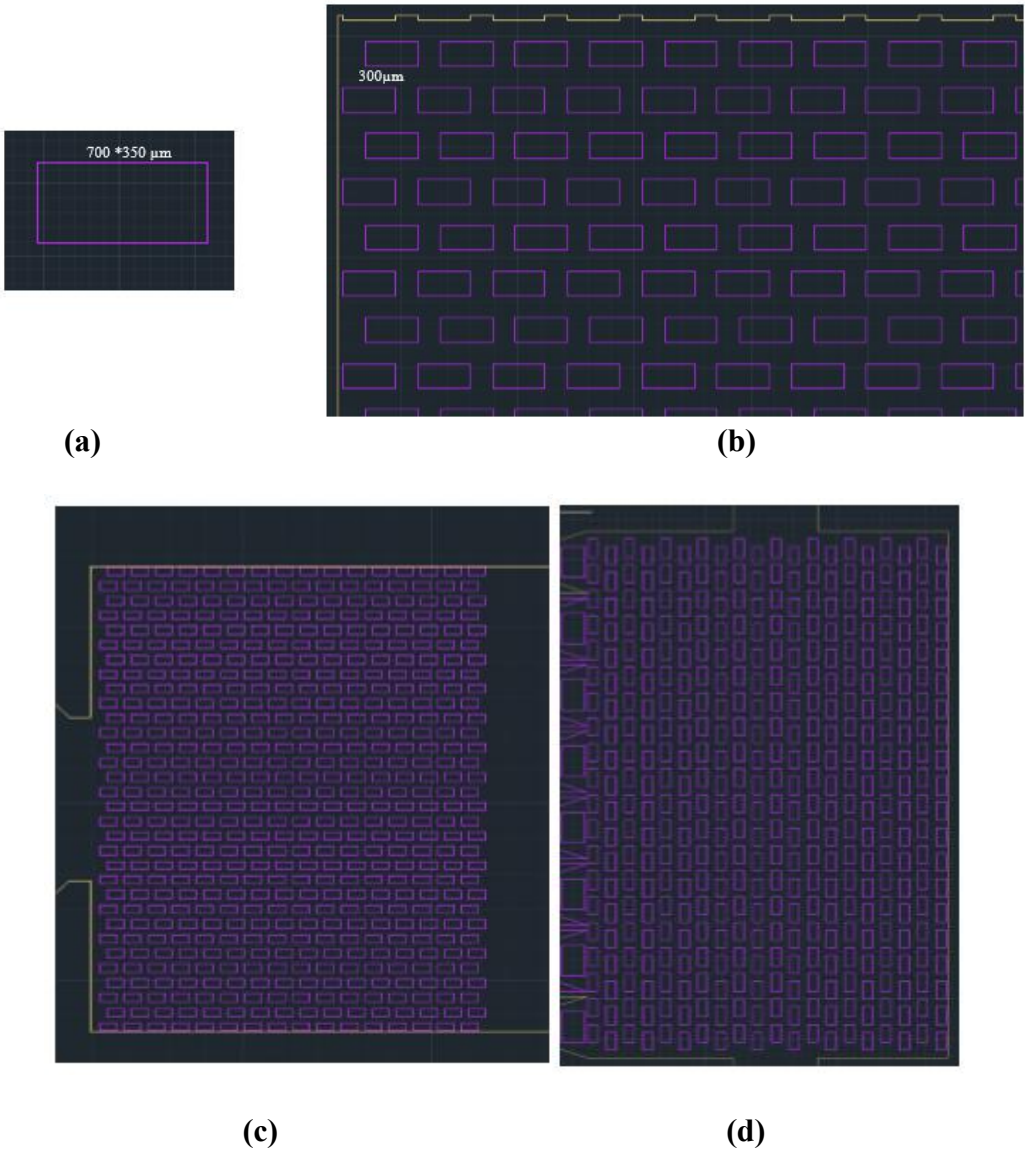

Figure 26**. (a) the pillar size. (b) the space between two array. (c) pump1. (d) pump 2.**

The schematic of mask 3 is shown in **Figure27(a)-(d)**. For pump 1, each array has 19 pillars and there is a total of 40 arrays. For pump 2, each array has 24 pillars and there is a total of 24 arrays.

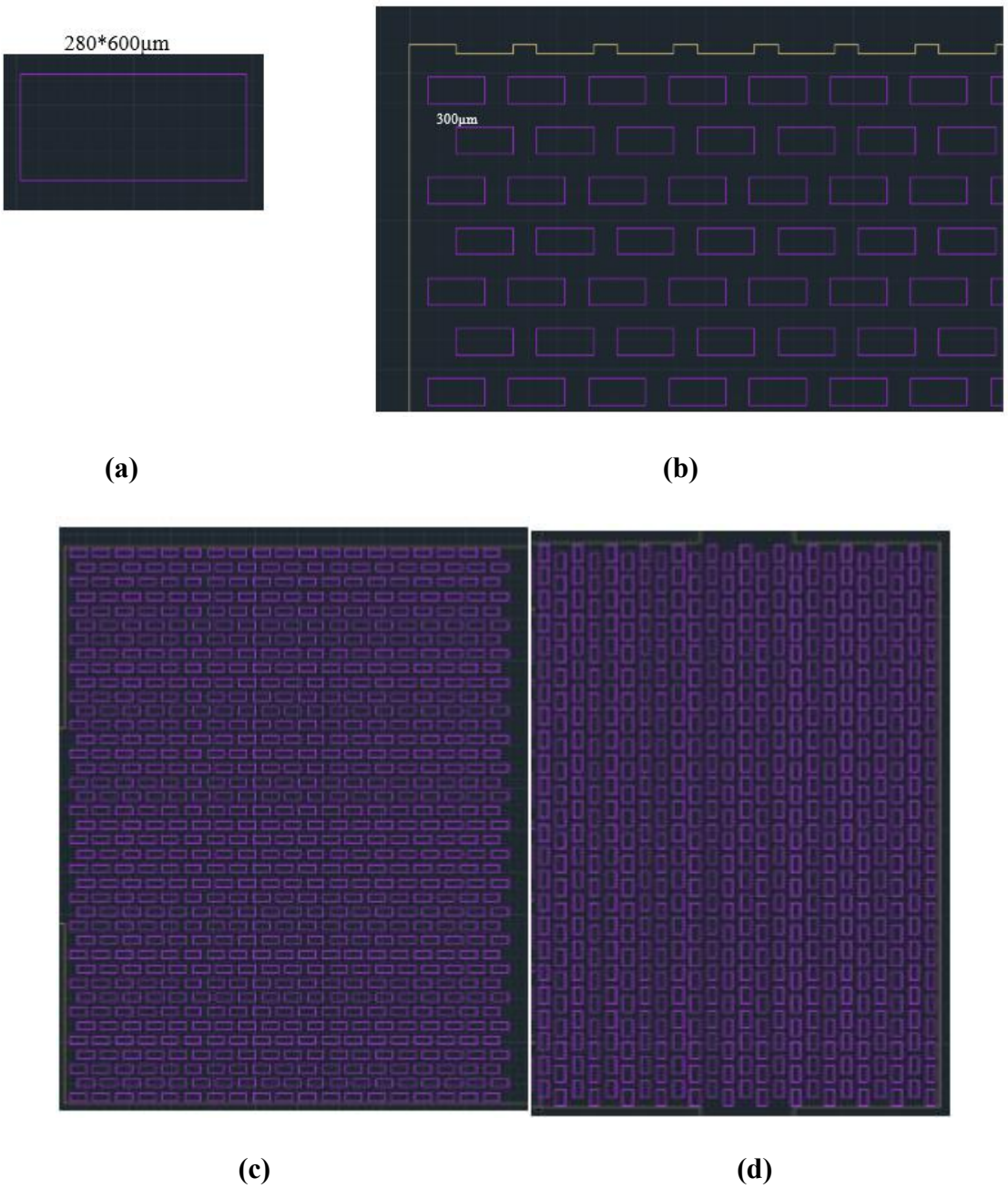

Figure 27**. (a) the pillar size. (b) the space between two array. (c) pump1. (d) pump 2.**

The schematic of mask 4 is shown in Figure28(a)-(d). For pump 1, each array has 24 pillars and there is a total of 70 arrays. For pump 2, each array has 31 pillars there is a total of 42 arrays.

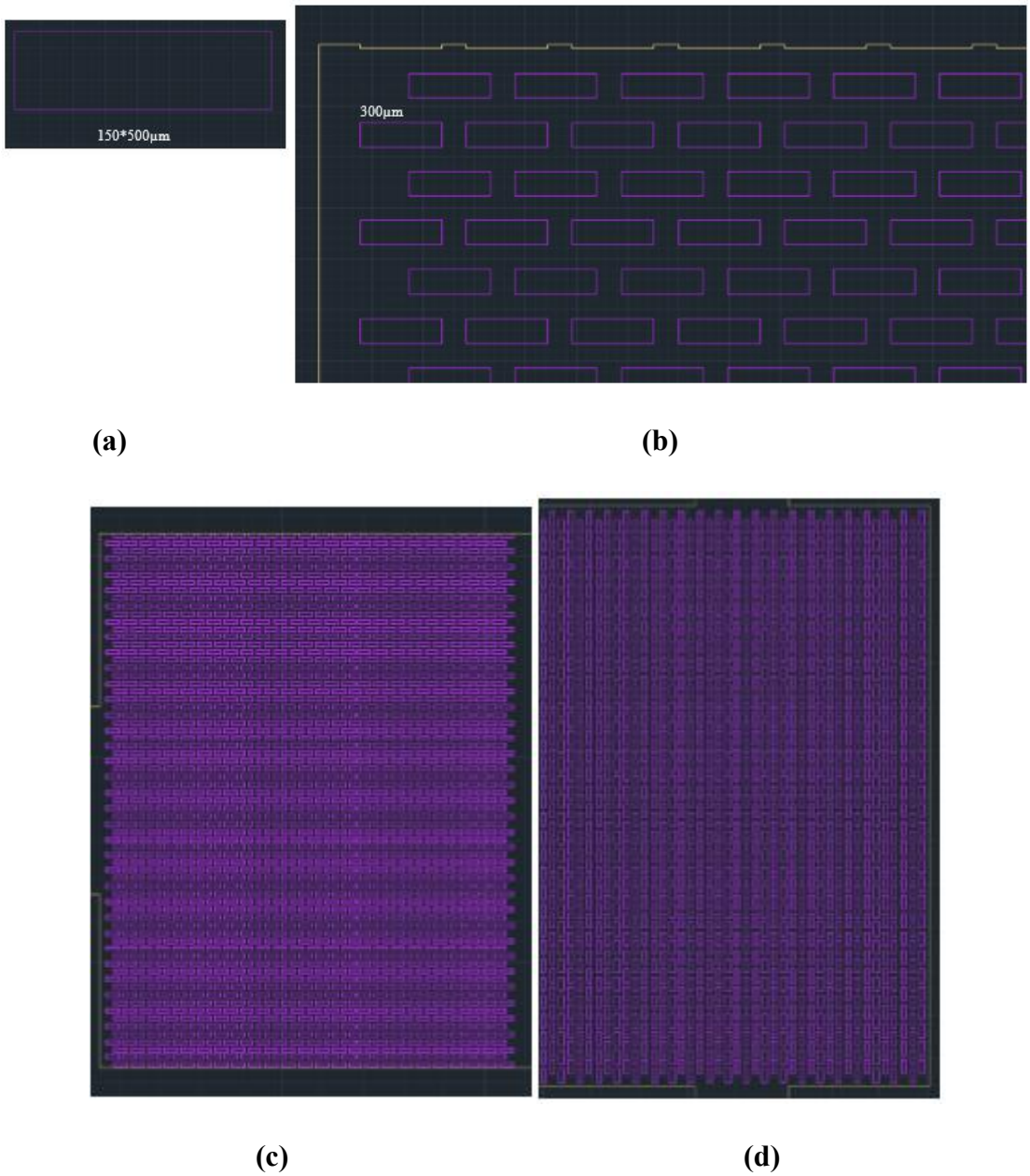

(a) **(b)**

(c) **(d)**

Figure 28**.(a) the pillar size. (b) the space between two array. (c) pump1. (d) pump 2.**

APPENDIX C. AAO FABRICATION

ITO glass substrates were purchased from Nanocs, Inc. The sheetresistance of the ITO on the glass is 100 X/sq. The photoresist AZ1512 and AZ developer were purchased from AZ Electronic Materialsplc. The following fluorescent dyes are purchased and used in theexperiments: Rhodamine 6G (R6G) (Lightning Powder,Inc.), fluorescein sodium salt (FSS) (Sigma, Inc.), fluorescein isothiocyanate(FITC) (Sigma, Inc.) and fluorescent brightening agents(FBA) (Sigma, Inc.).The detailed new fabrication process is illustrated in **Figure 29a**. TheITO glass substrate is washed thoroughly in four steps: by DI water, followed by Acetone, IPA, and DI water insequence. After a 5-minute baking of the cleaned ITO glass, a 2 lm thick aluminum layer is deposited by E-beam evaporationas shown in **Fig. 29b**. To achievesuccessful anodization the quality of the deposited Al is critical. One essential requirement is that the Alshould be totally oxide-free, meaning during E-beam evaporationany oxidation of Al must be avoided or, as found in our experiments, the as-depositedAl cannot be anodized.The other important requirement is the surface smoothness ofthe deposited Al. Measurements have a typical roughness inthe range of 6–12 nm [1-3], smooth enough for carryingout anodization, and not requiring further surface polishing . Thisis a significant advantage over carrying out anodizationon a commercial Al foil sheet, which usually requires several surface polishing steps to polish the surface of the Al sheet and ensure a sufficiently smooth surface [4].Then we carry out anodization process (either one-step or two-step)in acid solution (0.3 M oxalic acid) with 45 V DC voltage at 2 C to form AAO on the ITO glass substrate, as shown in **Figure. 29c**.In this step, a layer of AAO is formed over the whole substrate surface. Specifically,for the one-step anodization process to form AAO [5], weonly carry out one-step anodization on the samples for 25, 35,and 45 min, respectively. In contrast,

the two-step anodizationprocess to form AAO [4] takes 10 min for step-one anodizationin 0.3 M oxalic acid, followed by etching using a mixture ofphosphoric acid (0.4 M) and chromic acid (0.2 M) at 65 C for30 min, followed by a 40-minute step-two anodization in 0.3 Moxalic acid with the same experimental conditions as for step-oneanodization. The wafer is then vigorously rinsed in DI water, and a 150 nm thick aluminum layer is deposited on theAAO surface by thermal evaporation as shown in **Figure 29d**. Photolithographyis then performed on the Al-coated AAO substrate. Specifically,a 1 lm photoresist (AZ 1512) layer is spin-coated at4000 rpm on the substrate, then the coated substrate is soft bakedfor 50 s at 95 C. The micropatterns are then transferred and generatedon the photoresist through a photomask using a 416 nmlight exposure with a dose of 70 mJ/cm2, followed by a post-exposurebake for 50 s at 105 C. The exposed photoresist is developedand selectively removed by immersing in AZ developer for 25 s. Thepatterned AZ resist serves as a mask to protect the Al underneath.The patterns are then transferred to the Al layer by etchingthe unprotected Al area in an etching solution {(H3PO4:CH3-COOH:HNO3:H2O) 80:5:5:10 by weight%} for 35 s, as shown in**Figure. 29e**. During this step, care must be taken to avoid any overetchingof the Al since the patterned Al layer serves as the maskfor etching the AAO. The substrate is then immersed in a mixtureof phosphoric acid (0.4 M) and chromic acid (0.2 M) at 20 C for100 min to etch away the unprotected AAO and transfer the patternsinto the AAO layer, as shown in **Figure 29f**. Thereafter, the remainingphotoresist is washed away by dipping the substrate inacetone, followed by removing the Al layer using the Al etching solution.As a result, AAO micropatterns on the substrate areobtained as shown in **Figure. 29g**. Again, to obtain AAOmicropatterns with high fidelity, the steps for etching Al andAAO are critical, and the etching time should be optimized. Otherwise,the resulting AAO micropatterns might be either

over-etched orunder-etched. In addition, Al is chosen as the mask for the AAOlayer instead of the photoresist as described earlier since the thicknessof AAO is 2.5 lm [6-9]. It has been found that in mostcases the photoresist cannot serve as a robust mask due to the longetching time (100 min) of the AAO layer. As a result, the micropatternscannot be properly transferred directly from the photoresistto the AAO layer.

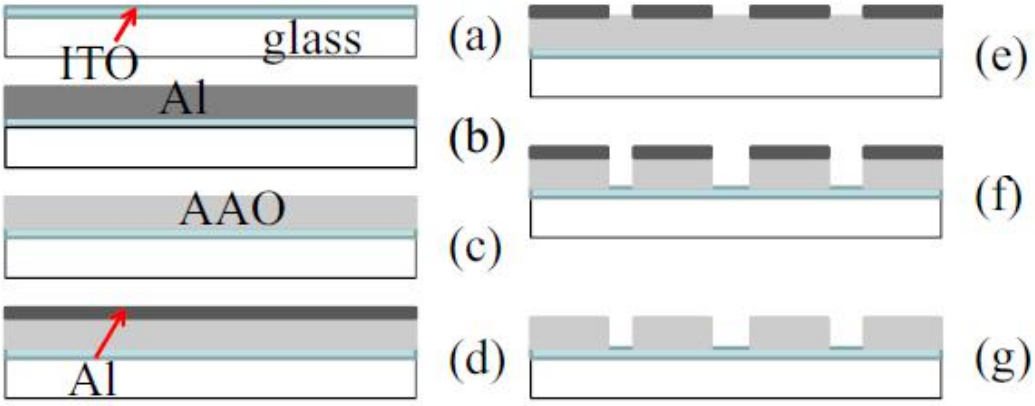

Figure 29.Sketch of the fabrication process flow for AAO micropatterns.

Reference

[1] X. Li, Y. He, T. Zhang, T. Lee, L. Que, Proc. IEEE NANO (2012), http://dx.doi.org/10.1109/NANO.2012.6321926.

[2] X. Li, Y. He, T. Zhang, L. Que, Opt. Express 20 (19) (2013) 21272–21277.

[3] X. Li, Y. He, L. Que, Langmuir 29 (7) (2013) 2439–2445.

[4] Y. He, X. Li, L. Que, J. Nanosci. Nanotechnol. 12 (10) (2012) 7915–7921.

[5] G. Sulka, S. Stroobants, V. Moshchalkov, G. Borghs, J.P. Celis, J. Electrochem. Soc. 149 (7) (2002) 97–103.

[6] E. Hourdakis, A.G. Nassiopoulou, IEEE Trans. Electron Devices 57 (10) (2010) 2679.

[7] E. Hourdakis, A.G. Nassiopoulou, Microelectron. Eng. 90 (2012) 12–14.

[8] A. Li, F. Muller, A. Birner, K. Nielsch, U. Gosele, Adv. Mater. 11 (1999) 483–487.

[9] H. Zhuo, F. Peng, L. Lin, Y. Qu, F. Lai, Thin Solid Films 519 (2011) 2308–2312.

ACKNOWLEDGEMENTS

I would really thank my major professor, Prof. Long, Que and my co-adviser Dr. Wei, Wang for your patience and kindness. You have been instrumental in motivating me to grow and succeed during graduate school; without you I would not have received an award for the one of the best 33 papers on IEEE-sensors.

Secondly, I need to thank my research group: Chao Song, Xiangchen Che, Shenming Gong, Pan Deng. Thanks for their support, suggestions, help, and critiques. Thanks to all of you for making my graduate career a pleasant one.

Thirdly, I would thank all of my friends from whom Ihave received love and encouragement.

Finally, I must say thanks for my parents. I love you!